nature portfolio

https://doi.org/10.1038/s41586-023-06692-3

Supplementary information

A resonant sextuplet of sub-Neptunes transiting the bright star HD 110067

In the format provided by the authors and unedited

Supplementary Information

Figures and Tables

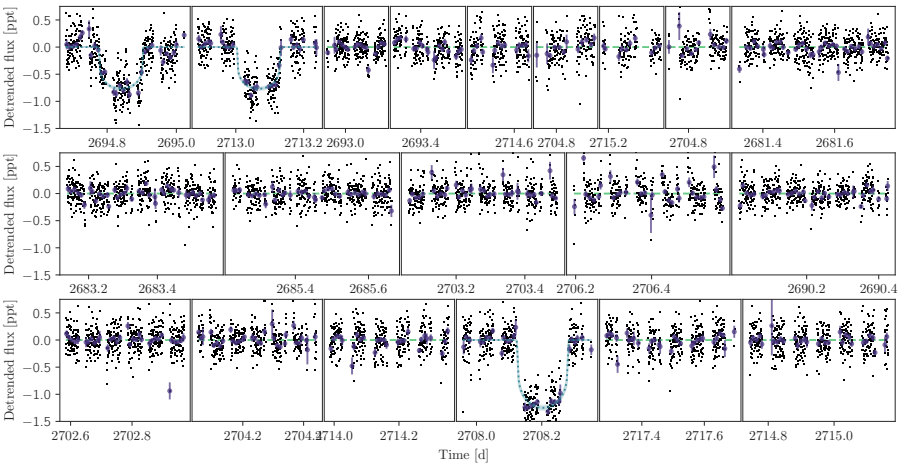

Fig. S1 Detrended CHEOPS photometry for all 19 visits. Time units are in TESS Julian Date (TJD ≡ BJD − 2457000), where BJD is the Barycentric Julian Date in units of days. Purple points show 15-minute bins. Dashed green lines show the best-fit planet models.

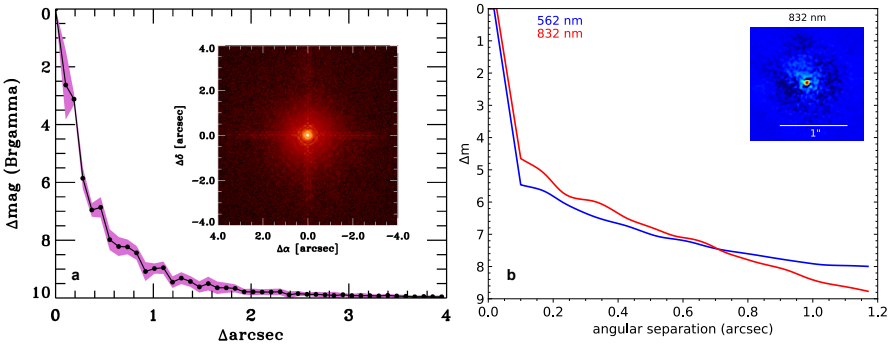

Fig. S2 High-resolution imaging data of HD 110067. a, Palomar NIR AO imaging and sensitivity curve for HD 110067 taken in the Br-γ filter. The image reaches a contrast of $\sim$ 8 mag fainter than the host star within 0.″5. The inset shows the image of the central portion of the data. **b,** Gemini optical speckle 5-sigma contrast curves for HD 110067 taken in the 562 nm and 832 nm bands. The images reach a contrast of $\sim$ 7 mag fainter than the host star within 0.″5. The inset shows the 832 nm reconstructed speckle image.

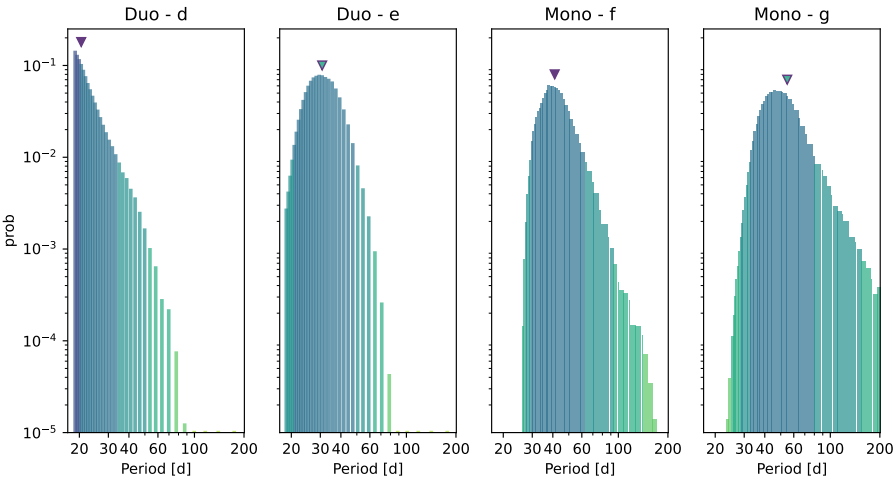

Fig. S3 Probability of each plausible orbital period for the two duo-transit and the two mono-transit events as fitted using `MonoTools`. The triangles mark the final planet periods; confirmed in the case of planets d and f, and predicted in the case of e and g.

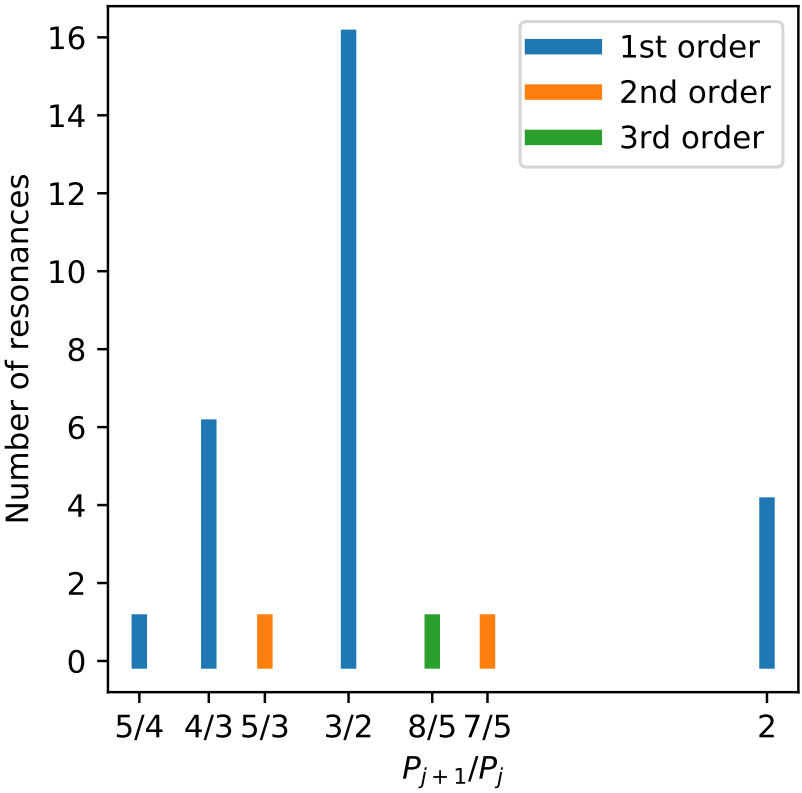

Fig. S4 Nearest MMRs of neighboring pairs of known chains of 3-body MMRs. The near-3:1 MMR of Kepler-221 is not shown here. The histogram shows an overabundance of first-order MMRs, especially with a period ratio of 3/2.

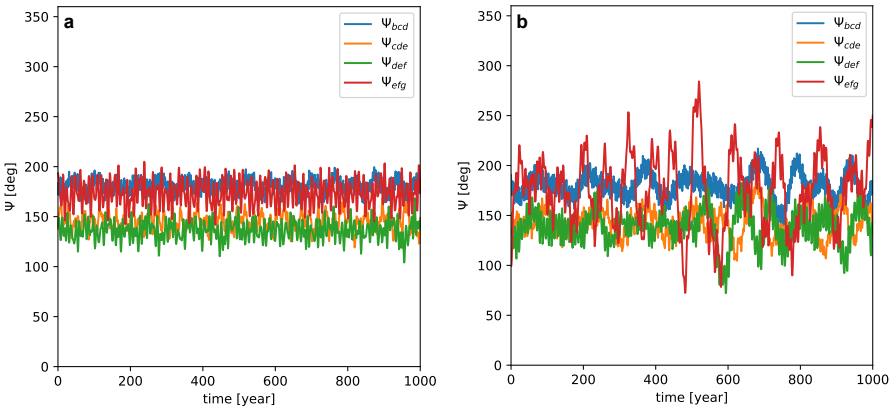

Fig. S5 N-body integration of 1000 years of evolution for the best initial conditions. a, case A2. **b,** case A0. The minimization of the function C was performed over the first 200 years only.

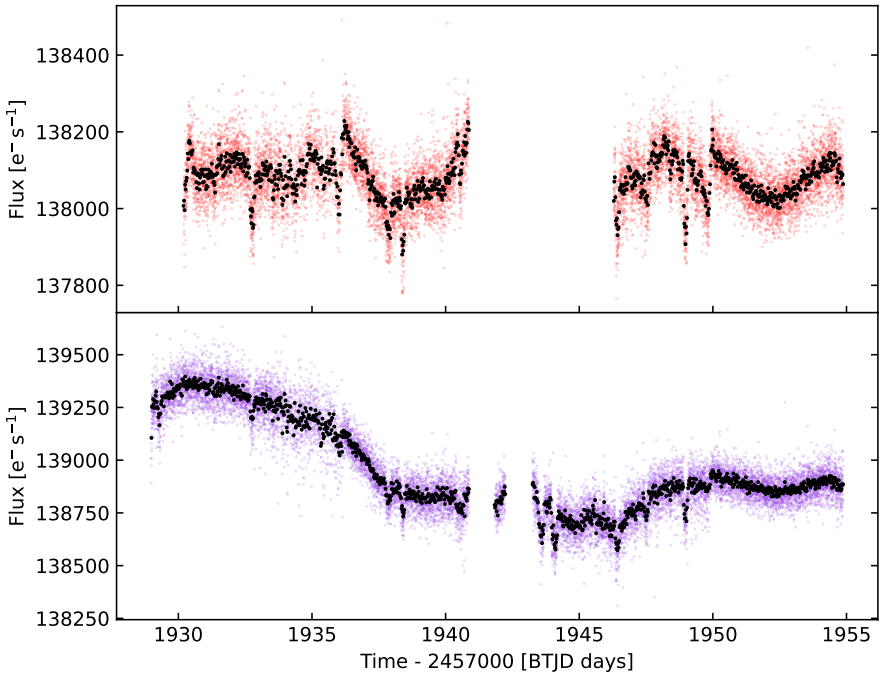

Fig. S6 TESS S23 light curves from different data reduction pipelines. The upper panel shows the PDCSAP light curve provided by SPOC in the MAST archive. The lower panel shows our custom extraction using pixel level decorrelation techniques. We are able to recover most of the data affected by scattered light and high background contamination from the Earth and the Moon discarded in the PDCSAP. The PLD-corrected data shows an additional transit of planet b and two single-transit events corresponding to planets f and g based on our dynamical analysis.

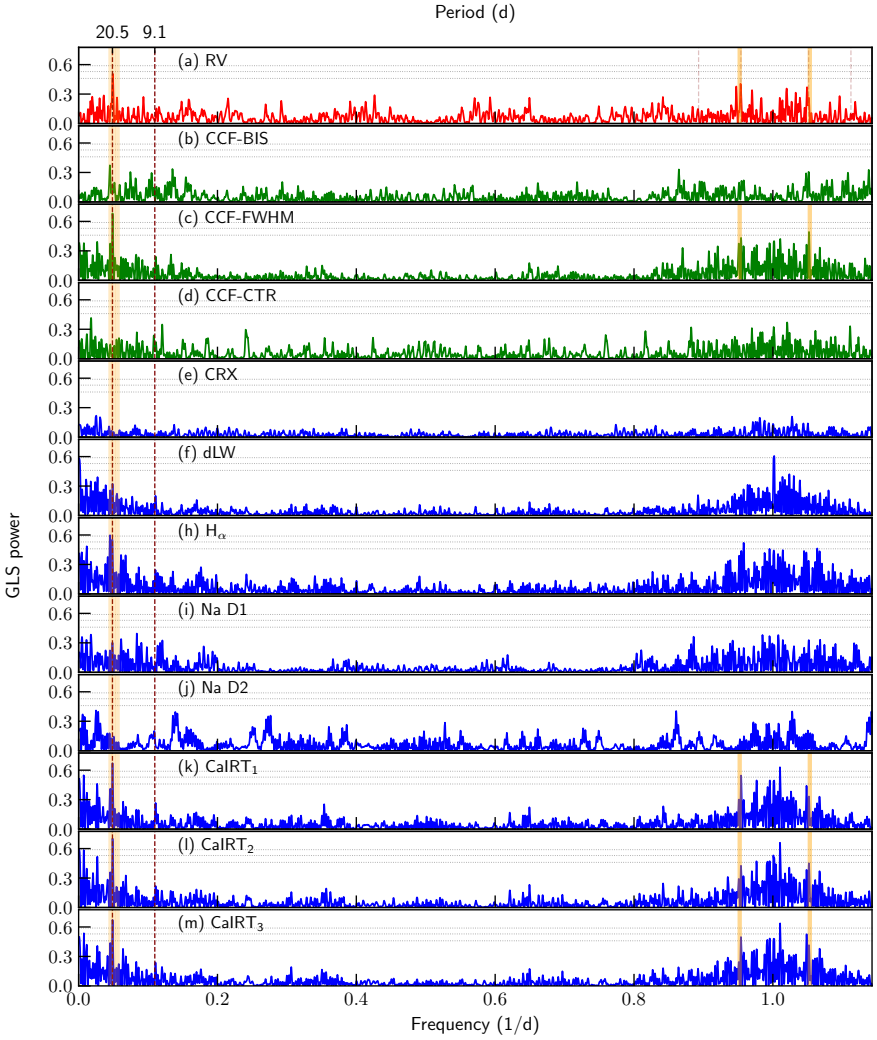

Fig. S7 GLS periodograms of CARMENES data. Signals from transiting planets HD 110067 b (f_b = 0.1097 d^{-1}, P_b ~ 9.11 d) and HD 110067 d (f_d = 0.0487 d^{-1}, P_c ~ 20.52 d) are marked as vertical dark-red dashed lines. Vertical, light-red dashed lines on panel (a) indicate 1-day aliases of planets b and d. The vertical orange solid lines mark the frequency of the stellar rotation period (f_{rot} = 0.0505 d^{-1}, P_{rot} = 19.8 ± 1 d) and its 1-day aliases. Panels plotted in green and blue show periodograms of spectral activity indicators measured with the CCF and template matching codes, respectively. Horizontal gray lines show the theoretical false alarm probability levels of 10 % (dotted line), 1 % (dashed line), and 0.1 % (dash-dotted line).

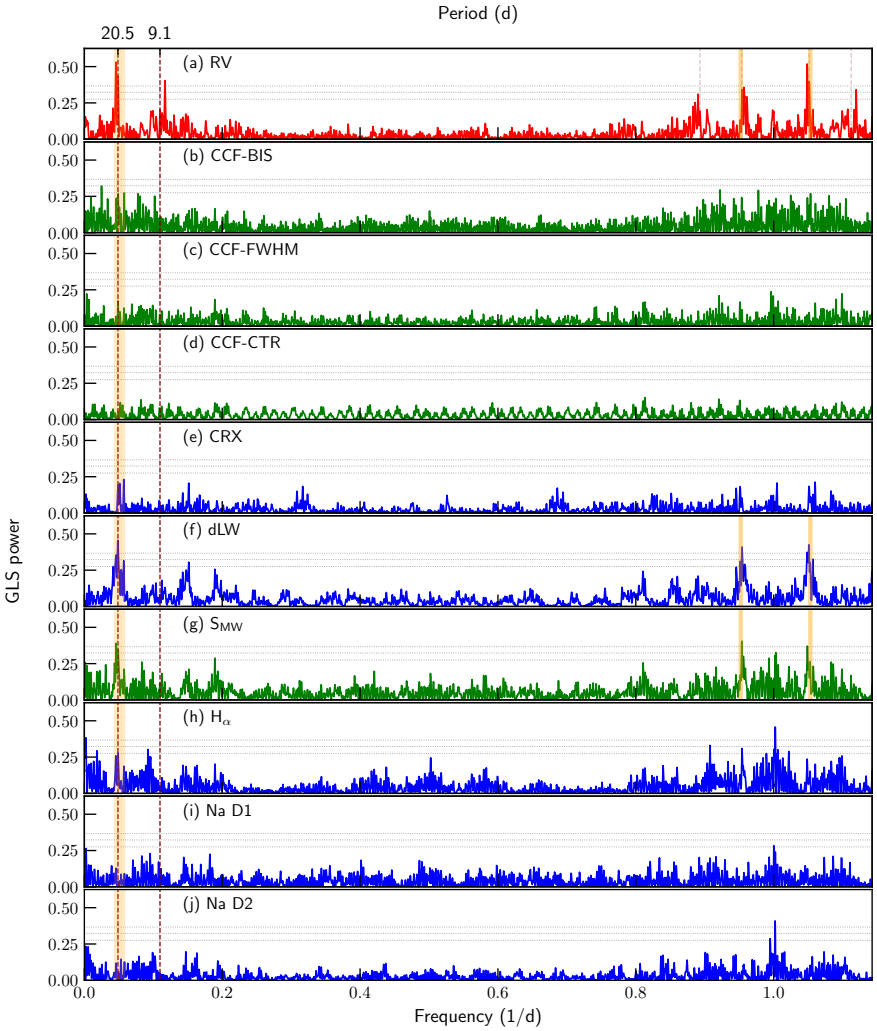

Fig. S8 GLS periodograms of HARPS-N data. Panels, lines, and colors as in Fig. S7.

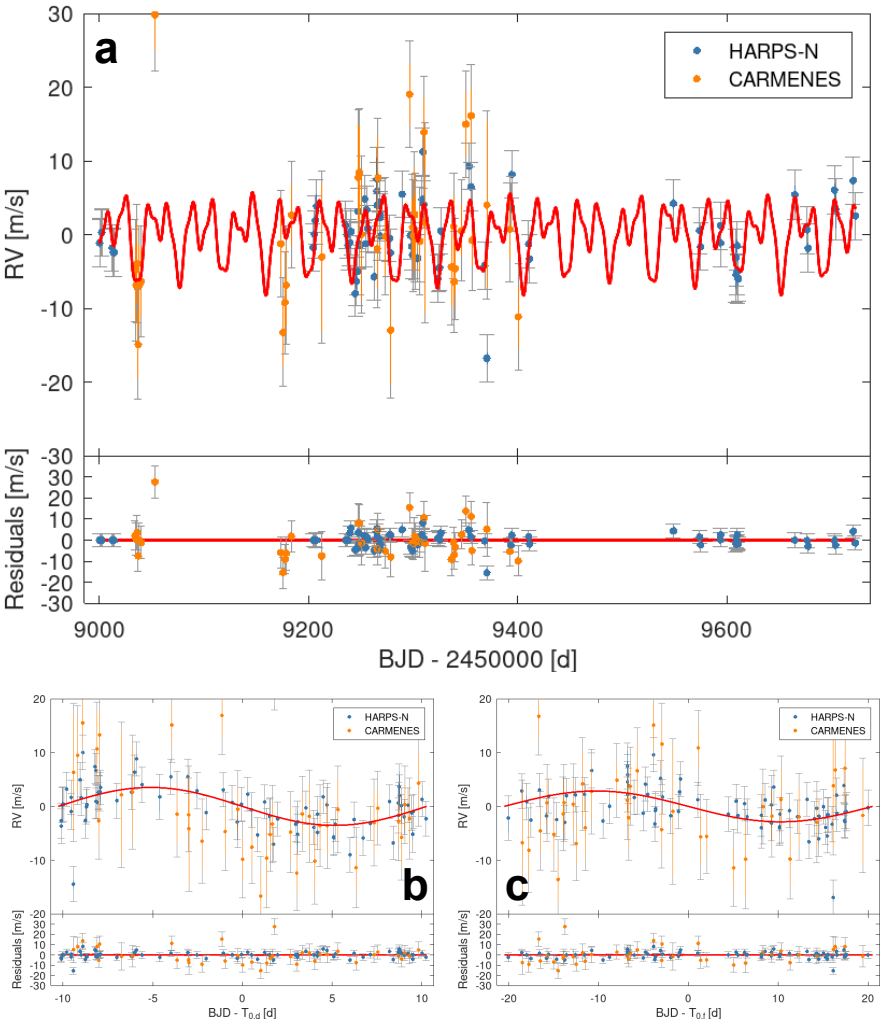

Fig. S9 RV time series with the corresponding best-fit model from Method I. a, full RV time series comprising the data points from both HARPS-N (blue) and CARMENES (orange). **b,c,** phase-folded time series showing the Keplerian signals of the two planets detected with high statistical confidence ($> 3\sigma$), HD 110067 d (**b**) and f (**c**). Radial velocity measurements are shown with solid circles with 1σ error bars with a gray error bar extension accounting for the inferred jitter.

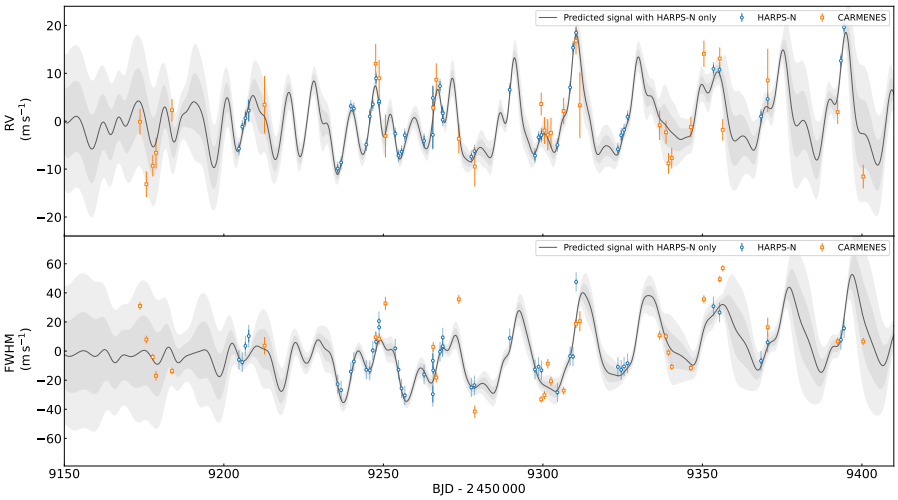

Fig. S10 Cross-validation analysis of the model from Method II. The two-dimensional GP model trained on HARPS-N only (blue circles) is shown as a solid black line indicating the median model, while light grey shaded areas show the 1σ and 2σ credible intervals of the predictive GP model. Error bars in the measurements indicate 1σ uncertainties.

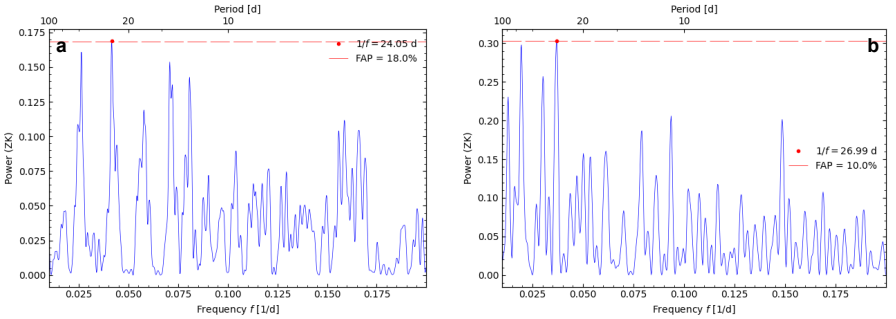

Fig. S11 Generalized Lomb-Scargle periodograms of the RV residuals obtained after subtracting the combined Keplerian signal of HD 110067 b, c, d, and f from the activity-cleaned RV time series. **a,** GLS periodogram computed from HARPS-N residuals. **b,** GLS periodogram computed from CARMENES residuals. Periodograms are normalized to unity. The highest peak and its false alarm probability (FAP) level are explicitly reported.

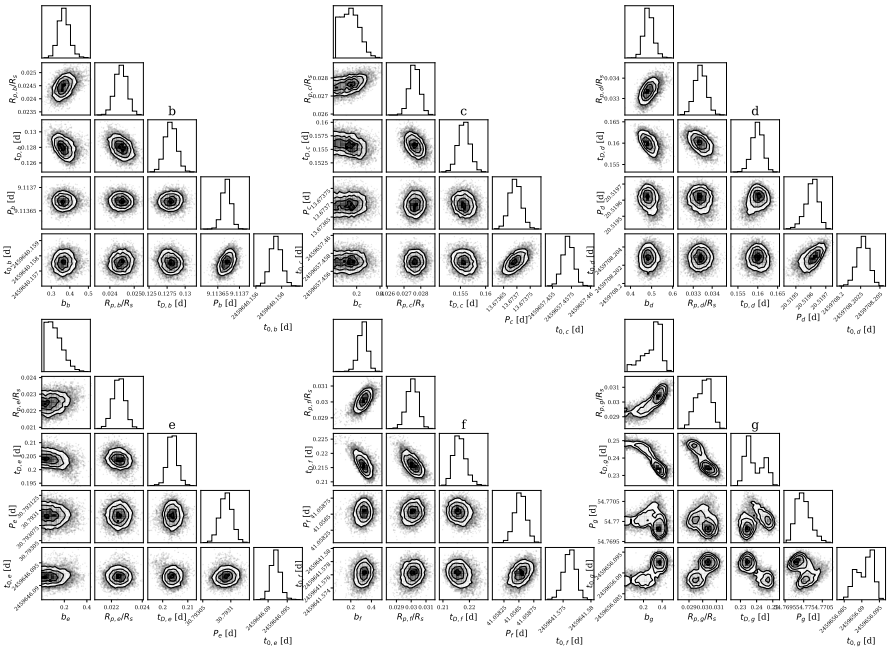

Fig. S12 Posterior distributions from the photometric fit. The top panels of the corner plot show the probability density function of each transit parameter. Contours are drawn to improve the visualization of the 2D histograms and indicate the 68.3%, 95.5%, and 99.7% confidence interval levels.

Table S1 Prior and posterior distributions for the TESS and CHEOPS photometric analysis. Error bars denote the 68% posterior credibility intervals.

Parameter	Unit	Prior	Posterior
Quadratic LD param. $u_{\rm TESS,1}$		$\mathcal{N}_{\mathcal{U}}(\mu=0.4,\sigma=0.1,a=0.0000,b=1.0000)$	0.472 ± 0.057
Quadratic LD param. $u_{\rm TESS,2}$		$\mathcal{N}_{\mathcal{U}}(\mu=0.21,\sigma=0.1,a=0.0000,b=1.0000)$	$0.171^{+0.085}_{-0.083}$
Quadratic LD param. $u_{\rm CHEOPS,1}$		$\mathcal{N}_{\mathcal{U}}(\mu=0.52,\sigma=0.1,a=0.0000,b=1.0000)$	0.435 ± 0.065
Quadratic LD param. $u_{\rm CHEOPS,2}$		$\mathcal{N}_{\mathcal{U}}(\mu=0.18,\sigma=0.1,a=0.0000,b=1.0000)$	$0.156^{+0.086}_{-0.081}$
Transit epoch $t_{0,\rm b}$	[TJD]	$\mathcal{N}(\mu=2640.16,\sigma=0.03)$	$2640.15797^{+0.00036}_{-0.00035}$
Orbital period $P_{\rm b}$	[d]	$\mathcal{N}_{\mathcal{U}}(\mu=9.1137,\sigma=0.0002,a=9.1129,b=9.1145)$	$9.113678 \pm 1e-05$
$\log R_{\rm b}/R_s$		$\mathcal{U}(a=-6.9,b=-2.3)$	$-3.6651^{+0.0095}_{-0.0095}$
Impact parameter $b_{\rm b}$		$\mathcal{U}(a=0.0,b=1+R_{p,b}/R_s)$	0.354 ± 0.033
Transit epoch $t_{0,\rm c}$	[TJD]	$\mathcal{N}(\mu=2657.45,\sigma=0.03)$	2657.45704 ± 0.0007
Orbital period $P_{\rm c}$	[d]	$\mathcal{N}_{\mathcal{U}}(\mu=13.6737,\sigma=0.0004,a=13.6723,b=13.6751)$	$13.673694 \pm 2.4e-05$
$\log R_{\rm c}/R_s$		$\mathcal{U}(a=-6.9,b=-2.3)$	-3.583 ± 0.012
Impact parameter $b_{\rm c}$		$\mathcal{U}(a=0.0,b=1+R_{p,c}/R_s)$	$0.16^{+0.079}_{-0.095}$
Transit epoch $t_{0,\rm d}$	[TJD]	$\mathcal{N}(\mu=2708.2,\sigma=0.03)$	$2708.20282^{+0.00074}_{-0.00079}$
Orbital period $P_{\rm d}$	[d]	$\mathcal{N}_{\mathcal{U}}(\mu=20.5196,\sigma=0.0006,a=20.5174,b=20.5218)$	$20.519617^{+3.8e-05}_{-4.8e-05}$
$\log R_{\rm d}/R_s$		$\mathcal{U}(a=-6.9,b=-2.3)$	$-3.4059^{+0.0090}_{-0.0093}$
Impact parameter $b_{\rm d}$		$\mathcal{U}(a=0.0,b=1+R_{p,d}/R_s)$	0.487 ± 0.023
Transit epoch $t_{0,\rm e}$	[TJD]	$\mathcal{N}(\mu=2646.09,\sigma=0.03)$	2646.0919 ± 0.0011
Orbital period $P_{\rm e}$	[d]	$\mathcal{N}_{\mathcal{U}}(\mu=30.79309,\sigma=1e-05,a=30.7889,b=30.7973)$	$30.793091 \pm 1.2e-05$
$\log R_{\rm e}/R_s$		$\mathcal{U}(a=-6.9,b=-2.3)$	-3.791 ± 0.018
Impact parameter $b_{\rm e}$		$\mathcal{U}(a=0.0,b=1+R_{p,e}/R_s)$	$0.104^{+0.09}_{-0.071}$
Transit epoch $t_{0,\rm f}$	[TJD]	$\mathcal{N}(\mu=2641.58,\sigma=0.03)$	2641.5763 ± 0.001
Orbital period $P_{\rm f}$	[d]	$\mathcal{N}_{\mathcal{U}}(\mu=41.0579,\sigma=0.0002,a=41.0520,b=41.0639)$	41.05854 ± 0.0001
$\log R_{\rm f}/R_s$		$\mathcal{U}(a=-6.9,b=-2.3)$	-3.498 ± 0.013
Impact parameter $b_{\rm f}$		$\mathcal{U}(a=0.0,b=1+R_{p,f}/R_s)$	0.339 ± 0.041
Transit epoch $t_{0,\rm g}$	[TJD]	$\mathcal{N}(\mu=2656.09,\sigma=0.03)$	$2656.0921^{+0.0013}_{-0.0031}$
Orbital period $P_{\rm g}$	[d]	$\mathcal{N}_{\mathcal{U}}(\mu=54.7693,\sigma=0.0002,a=54.7605,b=54.7780)$	$54.76992^{+0.00026}_{-0.00017}$
$\log R_{\rm g}/R_s$		$\mathcal{U}(a=-6.9,b=-2.3)$	$-3.493^{+0.014}_{-0.02}$
Impact parameter $b_{\rm g}$		$\mathcal{U}(a=0.0,b=1+R_{p,g}/R_s)$	$0.362^{+0.042}_{-0.09}$
TESS jitter $\log\sigma_{\rm TESS}$		$\mathcal{N}(\mu=-0.3,\sigma=1)$	-1.839 ± 0.042
CHEOPS jitter $\log\sigma_{\rm CHEOPS}$		$\mathcal{N}(\mu=-1.0,\sigma=3)$	-1.695 ± 0.033
Linear decorr. PR110048_TG028101 dy/dtime		$\mathcal{N}(\mu=0,\sigma=9.0)$	0.154 ± 0.012
Linear decorr. PR100031_TG052001 dy/dtime		$\mathcal{N}(\mu=0,\sigma=10.0)$	-0.074 ± 0.011
Linear decorr. shared param. dy/dbg		$\mathcal{N}(\mu=0,\sigma=0.4)$	0.0715 ± 0.0095
Linear decorr. shared param. dy/dcentroidx		$\mathcal{N}(\mu=0,\sigma=0.4)$	0.0055 ± 0.0077
Linear decorr. shared param. dy/dcentroidy		$\mathcal{N}(\mu=0,\sigma=0.4)$	-0.117 ± 0.013
Linear decorr. shared param. $dy/d\cos 2\Phi$		$\mathcal{N}(\mu=0,\sigma=0.4)$	-0.019 ± 0.058
Quadratic decorr. shared param. d^2y/dcentroidy^2		$\mathcal{N}(\mu=0,\sigma=0.4)$	0.0142 ± 0.0016
CHEOPS PR110048_TG028101 mean flux	[ppt]	$\mathcal{N}(\mu=-0.0,\sigma=0.6)$	0.25 ± 0.044
CHEOPS PR100031_TG052001 mean flux	[ppt]	$\mathcal{N}(\mu=-0.0,\sigma=0.4)$	$0.119^{+0.043}_{-0.045}$
CHEOPS PR100031_TG052002 mean flux	[ppt]	$\mathcal{N}(\mu=-0.0,\sigma=0.5)$	0.187 ± 0.044
CHEOPS rollangle B-spline 0	[ppt]	$\mathcal{N}(\mu=0,\sigma=0.2)$	0.48 ± 0.13
CHEOPS rollangle B-spline 1	[ppt]	$\mathcal{N}(\mu=0,\sigma=0.2)$	-0.23 ± 0.13
CHEOPS rollangle B-spline 2	[ppt]	$\mathcal{N}(\mu=0,\sigma=0.2)$	-0.17 ± 0.11
CHEOPS rollangle B-spline 3	[ppt]	$\mathcal{N}(\mu=0,\sigma=0.2)$	-0.06 ± 0.087
CHEOPS rollangle B-spline 4	[ppt]	$\mathcal{N}(\mu=0,\sigma=0.2)$	-0.138 ± 0.083
CHEOPS rollangle B-spline 5	[ppt]	$\mathcal{N}(\mu=0,\sigma=0.2)$	0.025 ± 0.078
CHEOPS rollangle B-spline 6	[ppt]	$\mathcal{N}(\mu=0,\sigma=0.2)$	-0.051 ± 0.081
CHEOPS rollangle B-spline 7	[ppt]	$\mathcal{N}(\mu=0,\sigma=0.2)$	0.052 ± 0.084
CHEOPS rollangle B-spline 8	[ppt]	$\mathcal{N}(\mu=0,\sigma=0.2)$	-0.039 ± 0.087
CHEOPS rollangle B-spline 9	[ppt]	$\mathcal{N}(\mu=0,\sigma=0.2)$	0.01 ± 0.091
CHEOPS rollangle B-spline 10	[ppt]	$\mathcal{N}(\mu=0,\sigma=0.2)$	-0.002 ± 0.097
CHEOPS rollangle B-spline 11	[ppt]	$\mathcal{N}(\mu=0,\sigma=0.2)$	0.07 ± 0.1
CHEOPS rollangle B-spline 12	[ppt]	$\mathcal{N}(\mu=0,\sigma=0.2)$	-0.14 ± 0.1
CHEOPS rollangle B-spline 13	[ppt]	$\mathcal{N}(\mu=0,\sigma=0.2)$	0.236 ± 0.098
CHEOPS rollangle B-spline 14	[ppt]	$\mathcal{N}(\mu=0,\sigma=0.2)$	-0.065 ± 0.093
CHEOPS rollangle B-spline 15	[ppt]	$\mathcal{N}(\mu=0,\sigma=0.2)$	$-0.057^{+0.085}_{-0.085}$
CHEOPS rollangle B-spline 16	[ppt]	$\mathcal{N}(\mu=0,\sigma=0.2)$	0.063 ± 0.082
CHEOPS rollangle B-spline 17	[ppt]	$\mathcal{N}(\mu=0,\sigma=0.2)$	-0.181 ± 0.084
CHEOPS rollangle B-spline 18	[ppt]	$\mathcal{N}(\mu=0,\sigma=0.2)$	0.153 ± 0.089
CHEOPS rollangle B-spline 19	[ppt]	$\mathcal{N}(\mu=0,\sigma=0.2)$	$-0.079^{+0.094}_{-0.096}$
CHEOPS rollangle B-spline 20	[ppt]	$\mathcal{N}(\mu=0,\sigma=0.2)$	0.1 ± 0.097
CHEOPS rollangle B-spline 21	[ppt]	$\mathcal{N}(\mu=0,\sigma=0.2)$	$-0.062^{+0.096}_{-0.094}$
CHEOPS rollangle B-spline 22	[ppt]	$\mathcal{N}(\mu=0,\sigma=0.2)$	-0.046 ± 0.093
CHEOPS rollangle B-spline 23	[ppt]	$\mathcal{N}(\mu=0,\sigma=0.2)$	$0.148^{+0.084}_{-0.089}$
CHEOPS rollangle B-spline 24	[ppt]	$\mathcal{N}(\mu=0,\sigma=0.2)$	-0.238 ± 0.079
CHEOPS rollangle B-spline 25	[ppt]	$\mathcal{N}(\mu=0,\sigma=0.2)$	-0.029 ± 0.078
CHEOPS rollangle B-spline 26	[ppt]	$\mathcal{N}(\mu=0,\sigma=0.2)$	0.316 ± 0.081
CHEOPS rollangle B-spline 27	[ppt]	$\mathcal{N}(\mu=0,\sigma=0.2)$	0.48 ± 0.12

Notes. $\mathcal{N}$ refers to a Normal prior, $\mathcal{U}$ a uniform prior, $\mathcal{N}_{\mathcal{U}}$ a bound Normal, and $\mathcal{I}$ to a prior interpolated from a transit-free GP fit.

Table S2 Priors and posterior distributions of the radial velocity fit model from Method I.

Parameter	Prior[(a)]	Final value[(b)]
HD 110067 b		
Orbital period P (days)	$\mathcal{N}(9.113667, 0.000011)$	9.113667 ± 0.000011
Transit epoch t_0 (d)	$\mathcal{N}(2640.15770, 0.00035)$	2640.15770 ± 0.00035
RV semi-amplitude K ($m\,s^{-1}$)	$\mathcal{U}[0, 10]$	< 3.3
HD 110067 c		
Orbital period P (days)	$\mathcal{N}(13.673692, 0.000022)$	13.673692 ± 0.000022
Transit epoch t_0 (d)	$\mathcal{N}(1932.75138, 0.00091)$	$1932.75138^{+0.00092}_{-0.00090}$
RV semi-amplitude K ($m\,s^{-1}$)	$\mathcal{U}[0, 10]$	< 2.0
HD 110067 d		
Orbital period P (days)	$\mathcal{N}(20.519638, 0.000044)$	20.519638 ± 0.000043
Transit epoch t_0 (d)	$\mathcal{N}(2646.64480, 0.00064)$	2646.64481 ± 0.00063
RV semi-amplitude K ($m\,s^{-1}$)	$\mathcal{U}[0, 10]$	3.8 ± 1.0
HD 110067 e		
Orbital period P (days)	$\mathcal{N}(30.79305, 0.00013)$	30.79305 ± 0.00013
Transit epoch t_0 (d)	$\mathcal{N}(2646.0922, 0.0016)$	2646.0922 ± 0.0016
RV semi-amplitude K ($m\,s^{-1}$)	$\mathcal{U}[0, 10]$	< 3.5
HD 110067 f		
Orbital period P (days)	$\mathcal{N}(41.057, 0.021)$	41.051 ± 0.021
Transit epoch t_0 (d)	$\mathcal{N}(2641.57770, 0.00094)$	$2641.57769^{+0.00095}_{-0.00094}$
RV semi-amplitude K ($m\,s^{-1}$)	$\mathcal{U}[0, 10]$	$2.28^{+0.69}_{-0.71}$
HD 110067 g		
Orbital period P (days)	$\mathcal{N}(54.743, 0.027)$	54.743 ± 0.027
Transit epoch t_0 (d)	$\mathcal{N}(2656.0955, 0.0011)$	2656.0955 ± 0.0011
RV semi-amplitude K ($m\,s^{-1}$)	$\mathcal{U}[0, 10]$	< 2.5
Other parameters		
HARPS-N RV jitter [$m\,s^{-1}$]	$\mathcal{U}[0, 100]$	$3.183^{+0.091}_{-0.067}$
CARMENES RV jitter [$m\,s^{-1}$]	$\mathcal{U}[0, 100]$	$5.89^{+0.15}_{-0.16}$

Footnotes. *(a)* $\mathcal{U}[a, b]$ refers to a uniform prior and $\mathcal{N}[a, b]$ to a Gaussian prior with mean a and standard deviation b. *(b)* Errors are defined as the 68.3% confidence interval of the posterior distribution. Upper limits correspond to 99% credible interval of the posterior distribution.

Table S3 Detrending parameters used in the radial velocity fit model from Method I.

Parameter	Value[(a)]
HARPS-N $\beta_{0,1}$ [10^7 m s^{-1}]	$-12.7^{+1.3}_{-1.2}$
HARPS-N $\beta_{1,t,1}$ [10^2 m s^{-1} yr^{-1}]	$-6.5^{+1.9}_{-1.7}$
HARPS-N $\beta_{2,t,1}$ [10^3 m s^{-1} yr^{-2}]	$25.1^{+3.8}_{-4.0}$
HARPS-N $\beta_{3,t,1}$ [10^4 m s^{-1} yr^{-3}]	$-7.9^{+1.2}_{-1.1}$
HARPS-N $\beta_{4,t,1}$ [10^3 m s^{-1} yr^{-4}]	$64.4^{+9.1}_{-9.4}$
HARPS-N $\beta_{1,F,1}$ [10^6 m s^{-1}/(km s^{-1})]	$54.8^{+5.3}_{-5.5}$
HARPS-N $\beta_{2,F,1}$ [10^5 m s^{-1}/(km s^{-1})^2]	$-79.8^{+8.0}_{-7.8}$
HARPS-N $\beta_{3,F,1}$ [10^4 m s^{-1}/(km s^{-1})^3]	$38.7^{+3.8}_{-3.9}$
HARPS-N $\beta_{1,\gamma,1}$ [10^4 m s^{-1}]	23.8 ± 2.4
HARPS-N $\beta_{2,\gamma,1}$ [10^5 m s^{-1}]	$95.9^{+9.7}_{-10.0}$
HARPS-N $\beta_{3,\gamma,1}$ [10^7 m s^{-1}]	12.7 ± 1.3
HARPS-N $\beta_{4,\gamma,1}$ [10^6 m s^{-1}]	$-14.0^{+1.5}_{-1.4}$
HARPS-N $\beta_{1,A,1}$ [10^3 m s^{-1}]	$74.6^{+8.9}_{-9.6}$
HARPS-N $\beta_{2,A,1}$ [10^2 m s^{-1}]	$-10.2^{+1.3}_{-1.2}$
HARPS-N $\beta_{1,R,1}$ [10 m s^{-1} dex^{-1}]	$35.8^{+2.4}_{-2.3}$
HARPS-N $\beta_{0,2}$ [10^6 m s^{-1}]	$-6.8^{+1.2}_{-1.0}$
HARPS-N $\beta_{1,t,2}$ [10 m s^{-1} yr^{-1}]	$-71.1^{+9.9}_{-9.7}$
HARPS-N $\beta_{2,t,2}$ [10^2 m s^{-1} yr^{-2}]	$8.9^{+1.2}_{-1.3}$
HARPS-N $\beta_{3,t,2}$ [10 m s^{-1} yr^{-3}]	$-46.2^{+6.9}_{-6.7}$
HARPS-N $\beta_{4,t,2}$ [10 m s^{-1} yr^{-4}]	$8.4^{+1.3}_{-1.4}$
HARPS-N $\beta_{1,F,2}$ [10^5 m s^{-1}/(km s^{-1})]	$29.4^{+4.4}_{-5.0}$
HARPS-N $\beta_{2,F,2}$ [10^4 m s^{-1}/(km s^{-1})^2]	$-42.2^{+7.1}_{-6.3}$
HARPS-N $\beta_{3,F,2}$ [10^3 m s^{-1}/(km s^{-1})^3]	$20.2^{+3.0}_{-3.4}$
HARPS-N $\beta_{1,\gamma,2}$ [10 m s^{-1}]	$28.8^{+8.3}_{-8.5}$
HARPS-N $\beta_{2,\gamma,2}$ [10^4 m s^{-1}]	0.7 ± 1.8
HARPS-N $\beta_{3,\gamma,2}$ [10^6 m s^{-1}]	-1.7 ± 1.4
HARPS-N $\beta_{4,\gamma,2}$ [10^7 m s^{-1}]	-4.5 ± 2.6
HARPS-N $\beta_{1,A,2}$ [10^2 m s^{-1}]	$-12.8^{+3.5}_{-3.2}$
HARPS-N $\beta_{2,A,2}$ [m s^{-1}]	$17.8^{+4.4}_{-4.9}$
HARPS-N $\beta_{1,R,2}$ [10 m s^{-1} dex^{-1}]	5.8 ± 1.9
CARMENES $\beta_{0,1}$ [10^2 m s^{-1}]	$0.5^{+2.0}_{-1.9}$
CARMENES $\beta_{1,F,1}$ [10 m s^{-1}/(km s^{-1})]	-5.1 ± 1.9
CARMENES $\beta_{1,\gamma,1}$ [10 m s^{-1} yr^{-2}]	$5.9^{+1.9}_{-1.7}$
CARMENES $\beta_{1,A,1}$ [m s^{-1} yr^{-3}]	$12.1^{+4.7}_{-4.6}$

Footnotes. *(a)* Errors are defined as the 68.3% credible interval of the posterior distribution.

Table S4 Parameters, priors, and posterior distributions of the radial velocity fit model from Method II.

Parameter	Prior[(a)]	Final value[(b)]
HD 110067 b		
Orbital period $P_{\rm orb}$ (days)	$\mathcal{N}[9.113678, 0.000010]$	$9.1136781^{+0.0000097}_{-0.0000099}$
Transit epoch t_0 (d)	$\mathcal{N}[2640.15797, 0.00036]$	$2640.15797^{+0.00037}_{-0.00035}$
RV semi-amplitude K (m s^{-1})	$\mathcal{U}[0, 10]$	$2.03^{+0.62}_{-0.65}$
HD 110067 c		
Orbital period $P_{\rm orb}$ (days)	$\mathcal{N}[13.673694, 0.000024]$	13.673693 ± 0.000024
Transit epoch t_0 (d)	$\mathcal{N}[2657.45704, 0.0007]$	$2657.45705^{+0.00068}_{-0.00071}$
RV semi-amplitude K (m s^{-1})	$\mathcal{U}[0, 10]$	< 1.55
HD 110067 d		
Orbital period $P_{\rm orb}$ (days)	$\mathcal{N}[20.519617, 0.00004]$	$20.519617^{+0.000040}_{-0.000039}$
Transit epoch t_0 (d)	$\mathcal{N}[2708.20282, 0.00080]$	$2708.20281^{+0.00069}_{-0.00070}$
RV semi-amplitude K (m s^{-1})	$\mathcal{U}[0, 10]$	$2.32^{+0.89}_{-0.88}$
HD 110067 e		
Orbital period $P_{\rm orb}$ (days)	$\mathcal{N}[30.793091, 0.000012]$	30.793091 ± 0.000012
Transit epoch t_0 (d)	$\mathcal{N}[2646.0917, 0.0011]$	2646.0919 ± 0.0011
RV semi-amplitude K (m s^{-1})	$\mathcal{U}[0, 10]$	< 0.80
HD 110067 f		
Orbital period $P_{\rm orb}$ (days)	$\mathcal{N}[41.05854, 0.0001]$	$41.058536^{+0.000100}_{-0.000096}$
Transit epoch t_0 (d)	$\mathcal{N}[2641.5763, 0.0010]$	$2641.57629^{+0.00100}_{-0.00098}$
RV semi-amplitude K (m s^{-1})	$\mathcal{U}[0, 10]$	$1.09^{+0.40}_{-0.42}$
HD 110067 g		
Orbital period $P_{\rm orb}$ (days)	$\mathcal{N}[54.76992, 0.00020]$	54.76992 ± 0.00020
Transit epoch t_0 (d)	$\mathcal{N}[2656.0921, 0.0020]$	$2656.0922^{+0.0019}_{-0.0020}$
RV semi-amplitude K (m s^{-1})	$\mathcal{U}[0, 10]$	< 1.3
GP hyperparameters		
GP Period $P_{\rm GP}$ (days)	$\mathcal{U}[19, 21]$	$19.80^{+0.14}_{-0.15}$
$\lambda_{\rm p}$	$\mathcal{U}[0.1, 2]$	$0.454^{+0.063}_{-0.048}$
$\lambda_{\rm e}$ (days)	$\mathcal{U}[10, 100]$	$46.91^{+7.04}_{-6.52}$
$A_{\rm RV}$ (m s^{-1})	$\mathcal{U}[-100, 100]$	$2.55^{+0.97}_{-0.84}$
$B_{\rm RV}$ (m s^{-1} d)	$\mathcal{U}[-100, 100]$	$19.3^{+3.8}_{-2.9}$
$A_{\rm FWHM}$ (m s^{-1})	$\mathcal{U}[0, 100]$	$25.9^{+4.7}_{-3.7}$
$B_{\rm FWHM}$ (m s^{-1} d)	$\mathcal{F}[0]$	0
Other parameters		
HARPS-N RV offset (km s^{-1})	$\mathcal{U}[-0.5134, 0.5161]$	$-0.00354^{+0.00089}_{-0.00080}$
HARPS-N RV jitter (m s^{-1})	$\mathcal{J}[0.1, 100]$	$1.14^{+0.42}_{-0.49}$
HARPS-N FWHM offset (km s^{-1})	$\mathcal{U}[6.3466, 7.4636]$	$6.8941^{+0.0076}_{-0.0073}$
HARPS-N FWHM jitter (m s^{-1})	$\mathcal{J}[0.1, 100]$	$6.47^{+0.85}_{-0.74}$
CARMENES RV offset (km s^{-1})	$\mathcal{U}[-9.2768, -8.2468]$	$-8.7636^{+0.0011}_{-0.0010}$
CARMENES RV jitter (m s^{-1})	$\mathcal{J}[0.1, 100]$	$1.33^{+1.06}_{-0.95}$
CARMENES FWHM offset (km s^{-1})	$\mathcal{U}[7.0443, 8.1796]$	$7.6235^{+0.0078}_{-0.0077}$
CARMENES FWHM jitter (m s^{-1})	$\mathcal{J}[0.1, 100]$	$14.35^{+2.26}_{-1.93}$

Footnotes. *(a)* $\mathcal{F}[a]$ refers to a fixed value a and $\mathcal{J}[a, b]$ to the modified Jeffrey's prior. *(b)* Upper limits correspond to 99% credible interval of the posterior distribution.

Table S5 Gas mass fraction for each planet resulting from the internal structure model. The indicated values are the median, as well as the 5 and 95 % percentiles of the distribution.

Planet	$\log(M_{\rm gas})_{\rm Method\ I}$	$\log(M_{\rm gas})_{\rm Method\ II}$
HD 110067 b	$-2.52^{+0.66}_{-1.65}$	$-3.00^{+1.16}_{-3.66}$
HD 110067 c	$-2.32^{+0.50}_{-1.04}$	$-2.13^{+0.44}_{-0.81}$
HD 110067 d	$-0.92^{+0.37}_{-0.59}$	$-0.97^{+0.32}_{-0.37}$
HD 110067 e	$-6.55^{+3.94}_{-4.91}$	$-2.95^{+0.52}_{-0.73}$
HD 110067 f	$-2.28^{+1.21}_{-7.78}$	$-1.44^{+0.34}_{-0.41}$
HD 110067 g	$-1.39^{+0.40}_{-1.03}$	$-1.52^{+0.42}_{-1.06}$